Chapter 14
Building the Machines: Scaffolding Protein Functions During Bacteriophage Morphogenesis

Peter E. Prevelige and Bentley A. Fane

Abstract For a machine to function, it must first be assembled. The morphogenesis of the simplest icosahedral virus would require only 60 copies of a single capsid protein to coalesce. If the capsid protein's structure could be entirely dedicated to this endeavor, the morphogenetic mechanism would be relatively uncomplicated. However, capsid proteins have had to evolve other functions, such as receptor recognition, immune system evasion, and the incorporation of other structure proteins, which can detract from efficient assembly. Moreover, evolution has mandated that viruses obtain additional proteins that allow them to adapt to their hosts or to more effectively compete in their respective niches. Consequently, genomes have increased in size, which has required capsids to do likewise. This, in turn, has lead to more complex icosahedral geometries. These challenges have driven the evolution of scaffolding proteins, which mediate, catalyze, and promote proper virus assembly. The mechanisms by which these proteins perform their functions are discussed in this review.

14.1 Introduction

The so-called spherical viral capsids have underlying icosahedral symmetry. While a true icosahedron is composed of 60 strictly equivalent subunits, viral capsids with true icosahedral or $T=1$ symmetry are relatively rare, presumably because the internal volume of $T=1$ particles is constrained. Instead, most "spherical" viruses are subtriangulated icosahedra with triangulation (T) numbers corresponding to a mathematical progression put forth by Caspar and Klug (Caspar and Klug 1962). For capsids with T numbers greater than 1, the subunits do not occupy identical positions within the lattice. This, in turn, leads to pathway-dependent self-assembly (Rossmann 1984). For many smaller viruses, all the information required for high fidelity assembly can be encoded, or self-contained, entirely in the coat protein subunits. However, larger viruses or small viruses upon which unique evolutionary constraints have been imposed frequently require additional proteins to insure robust assembly. Among those proteins are the "scaffolding" proteins, a class of auxiliary proteins that are present

P.E. Prevelige (✉)
Department of Microbiology, University of Alabama at Birmingham,
BBRB 416/6, 845 19th St. South, Birmingham, AL 35294-2170, USA
e-mail: prevelig@uab.edu

B.A. Fane
Department of Plant Sciences, The BIO5 Institute, University of Arizona,
Keating Building, 1657 E. Helen Street, Tucson, AZ 85721, USA

M.G. Rossmann and V.B. Rao (eds.), *Viral Molecular Machines*,
Advances in Experimental Medicine and Biology 726, DOI 10.1007/978-1-4614-0980-9_14,

transiently during assembly and are not part of the final structure. Although common, scaffolding proteins are not ubiquitous. Most plant viruses and small, enveloped animal viruses do not require them. In general, these coat proteins have not been constrained by the evolution of a receptor-binding domain or domains that recruit or interact with other structural proteins. As coat proteins evolved to perform additional functions, efficient assembly may have become compromised. Thus, additional adaptations may have become required. Scaffolding proteins constitute only one of these adaptations; coat proteins have evolved as well. In some systems, best represented by the parvoviruses, maximal infectivity and/or fitness most likely requires constructing capsids with two or three coat protein variants (Hernando et al. 2000). The $P=3$ picornavirus capsids represent a more complex example: capsids contain three unique coat proteins, which share similar structures and a common evolutionary origin (Hogle et al. 1985; Verlinden et al. 2000). And finally, the nodaviruses and caliciviruses coat proteins have evolved large exterior domains that may function in receptor binding and immune evasion (Chen et al. 2006; Tang et al. 2006).

Several factors may have driven the evolution of scaffolding proteins. These include increases in genome size and the need to interact with minor capsid components. As genomes enlarged, capsids enlarged as well, creating virions with larger T numbers and/or prolate morphologies. However, the coat proteins of large icosahedral viruses can still form capsids of smaller T numbers. Similarly, those found in prolate heads can form icosahedral structures. Moreover, most coat proteins will form aberrant capsid-like structures if left to their own devices. Therefore, a mechanism to ensure morphogenetic fidelity, vis-à-vis proper capsid size and shape formation, had to evolve, and this mechanism most often included scaffolding proteins. The need to rapidly assemble capsids before cell death and/or programmed cell lysis may also have contributed to their evolution. This contribution of this factor is most apparent with the microviruses, ostensibly simple viruses that accomplish an almost unimaginable fast replication cycle by employing two-scaffolding proteins.

14.2 Bacteriophage P22

14.2.1 The Assembly Pathway of Bacteriophage P22

The assembly pathway of the *Salmonella typhimurium* bacteriophage P22 is typical of the double-stranded (ds) DNA bacteriophages (Fig. 14.1). The first identifiable structural intermediate is a "procapsid" (King et al. 1973) composed of an outer shell of 415 molecules of the 47-kDa coat protein (the product of gene 5), arranged with $T=7$ symmetry. The procapsid does not contain nucleic acid. Instead, it contains a core composed of ~300 molecules of the 33-kDa scaffolding protein (encoded by gene 8). Biochemical and genetic studies demonstrated that in addition to scaffolding protein, the procapsid contains approximately 12 copies of the portal protein (the product of gene 1) and 12–20 copies of each of the pilot and ejection proteins (the products of genes 7, 16, and 20). All of these proteins are required for productive infection (Casjens and King 1974). In addition to promoting the fidelity of coat protein assembly, the results of genetic studies implicate the P22 scaffolding protein in the incorporation of these minor capsid proteins (Weigele et al. 2005). Scaffolding-dependent minor capsid protein incorporation is observed in many assembly systems, suggesting a common force driving their evolution.

One fivefold symmetrical vertex of the icosahedron is differentiated from the other 11 by the presence of a dodecameric portal protein complex. Structural studies indicate that the core of the portal protein is conserved among phages P22, Phi29, and SPP1 (Kang et al. 2008; Lander et al. 2009; Lebedev et al. 2007; Simpson et al. 2000). This conservation appears to extend even to the herpesviruses (Baker et al. 2005). DNA is packaged through this portal vertex. A terminase complex

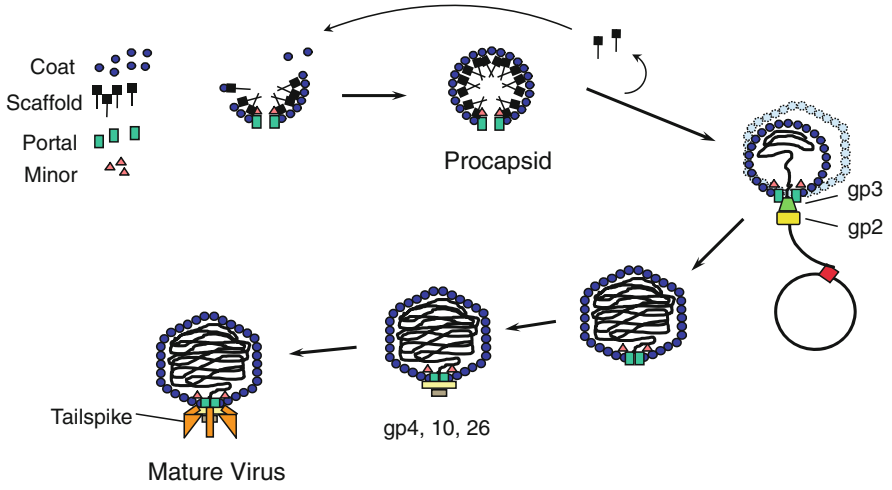

Fig. 14.1 The assembly pathway of bacteriophage P22. The initial structure formed, the procapsid, is assembled by the copolymerization of 415 molecules of the coat protein with approximately 300 molecules of the scaffolding protein. The portal and minor proteins are incorporated at this stage. The DNA is replicated as a concatemer. The terminase proteins (gp2 and gp3) bind to the DNA to deliver it to the portal vertex. The DNA is packaged by a headful mechanism in an ATP-dependent process. DNA packaging results in scaffolding protein exit. The released scaffolding protein can function in additional rounds of assembly. Packaging results in an expansion of the capsid and an increase in angularity. The portal vertex is closed by the binding of the products of gene 4, 10, and 26. Finally, attachment of the tailspike trimers renders the phage infectious

composed of multiple copies of two proteins is responsible for recognizing a "pac" sequence on the DNA, delivering the DNA to the portal vertex, and driving chemomechanical translocation through ATP hydrolysis (Rao and Feiss 2008). DNA packaging results in an approximately 10% expansion of the $T=7$ lattice, a pronounced increase in stability, and the egress of the scaffolding protein (Jiang et al. 2003; Kang and Prevelige 2005). In P22 and the *Bacillus subtilis* phage Phi29, the scaffolding protein exits intact and can be recycled in further rounds of assembly (Bjornsti et al. 1983; King and Casjens 1974). In most other dsDNA-containing bacteriophage and in herpesviruses, cleavage of the scaffolding protein by a virally encoded protease facilitates its removal.

14.2.2 The Role of the P22 Scaffolding Protein

In wild-type P22 infections, approximately 30 min postinfection, the cells burst and typically release approximately 500 newly formed virus particles. In cells infected with mutants that block DNA packaging, such as those with defective terminase proteins, the cells accumulate large numbers of procapsids within this time frame without evidence of partially formed shells (Lenk et al. 1975). In contrast, when cells are infected with mutants that prevent the synthesis of functional scaffolding protein, very few particles are produced. If infections are allowed to proceed long past the normal lysis time, aberrant particles, including small shells and spirals, accumulate (Earnshaw and King 1978). The morphology of the spirals, which constitute ~45% of the population by mass, suggests that they have an incorrect radius of curvature, which may be due to the improper positioning of the pentameric vertices. From these simple observations, two of the key functions of scaffolding protein can be discerned. Scaffolding protein promotes assembly, somehow lowering the concentration of coat protein required for polymerization, as evinced by the slower in vivo kinetics of aberrant particle formation, and ensures the fidelity of form determination.

14.2.3 Structural Studies of P22 Scaffolding Function

Biochemical and structural investigations have focused on two general phenomena: (1) the mechanism by which the P22 scaffolding protein imparts form determining information and (2) the mechanism by which it catalyzes assembly. The results of small angle X-ray diffraction (SAXS) experiments with procapsids indicated that the scaffolding protein density can be modeled as a thick shell or solid ball contained within the procapsid (Earnshaw et al. 1976). However, the results of subsequent biochemical experiments demonstrated that this core was formed during assembly and did not act as a template onto which the coat protein polymerized (Prevelige et al. 1988). Three-dimensional cryo-electron image reconstructions of P22 proheads elucidated the structure of these cores, revealing that the scaffolding protein was not packed with overall icosahedral symmetry (Thuman-Commike et al. 1996). Rather scaffolding protein interacts with the coat protein in a defined way only at the inside edge of the coat protein shell and the regions of ordered density falls off rapidly, presumably due to scaffolding flexibility. A similar situation is seen in herpesviruses where the scaffolding appears to be icosahedrally ordered only at the points of contact with the coat protein shell (Zhou et al. 1998). Thus, scaffolding proteins may impart form determining information through local interactions, for it is difficult to imagine how icosahedral information can pass through randomly oriented molecules, and indeed, a "local rules"-based model of how scaffolding protein can direct assembly has been proposed (Berger et al. 1994).

14.2.4 Kinetic Studies of P22 Scaffolding Function

Dissecting the assembly pathway demands a kinetic approach. Toward this end substantial progress has been made with a P22 in vitro assembly system in which purified coat and scaffolding protein subunits form procapsid-like particles with high yield and fidelity (Prevelige et al. 1988). The results of in vitro assembly experiments have demonstrated that (1) procapsid morphogenesis is a nucleation-limited process (Prevelige et al. 1993) and (2) that the pathway of assembly is well directed (Prevelige et al. 1993). Approximately 120 molecules of scaffolding protein are required for procapsid assembly (Prevelige et al. 1988). Scaffolding protein dimers are the dominant active form in assembly (Parker et al. 1997). However, monomers are required for completion of assembly (Tuma et al. 2008). Thus, scaffolding is required not just to nucleate assembly but throughout the assembly process. In the absence of monomeric scaffolding protein, assembly appears to become kinetically trapped leading to the production of partially formed shells. Full elongation can be achieved by the subsequent addition of monomeric scaffolding protein. Kinetic trapping can also be achieved by decreasing the ionic strength which favors the electrostatic coat/scaffolding interaction (Parent et al. 2005). In this case, completion can be achieved by increasing the salt concentration (Parent et al. 2005). Collectively, these experimental results fit nicely with the observation that the scaffolding protein is a weak monomer–dimer–tetramer association system (Parker et al. 1997) and suggest that the proper balance between nucleation and growth is maintained through the distribution of scaffolding oligomers.

14.2.5 The Structure of the P22 Scaffolding Protein

Although attempts to crystallize the P22 scaffolding protein have not been fruitful, other biophysical characterizations have provided some structural insights. The results of hydrodynamic studies indicate it is an extended, rod-like molecule (Fuller and King 1980), and the results of circular dichroism

Fig. 14.2 The structure of the coat protein-binding domain of the P22 scaffolding protein. The NMR structure of the C-terminal coat protein-binding domain of P22 scaffolding protein (residues 264–303) is shown as a *ribbon diagram* (PDB 1gp8). The lysine and arginine side chains are shown in stick representation

studies indicate that it is highly α-helical (Tuma et al. 1998). Analytical ultracentrifuge analyses under assembly conditions have demonstrated that it is a monomer–dimer–tetramer self-associating system in solution (Parker et al. 1997). The Phi29 and SPP1 internal scaffolding proteins also dimerize (Morais et al. 2003; Poh et al. 2008) as do the øX174 and P4 external scaffolding proteins (Marvik et al. 1995; Morais et al. 2004). Evidence for a physiological role for oligomerization comes from in vitro assembly experiments. Kinetic analysis of the rate of assembly as a function of scaffolding protein concentration suggested that assembly displayed a kinetic order of between 1.7 and 3.5 with regard to scaffolding protein (Prevelige et al. 1993) and the isolation of a naturally occurring mutant (R74C/L177I) that spontaneously formed disulfide cross-linked dimers allowed for the direct testing of dimers in assembly reactions (Parker et al. 1997). The rate of assembly with covalently dimeric scaffolding protein was significantly faster than with an equivalent concentration of wild-type scaffolding protein suggesting an active role for dimers in assembly. While the regions of the scaffolding protein responsible for oligomerization remain undefined, there is some mutational data that bears on this question. The fact that the R74C mutation leads to the spontaneous formation of disulfide cross-linked dimers suggests that the dimers are likely symmetrical with amino acid 74 located near the dimer interface. A scaffolding protein mutant in which the N-terminal 140 amino acids were deleted was capable of promoting assembly. Analytical ultracentrifugation experiments indicated that this protein was capable of dimerization but not tetramerization, suggesting that tetramerization may not be critical during assembly (Tuma et al. 1998; Weigele et al. 2005).

Protein dissection experiments indicated that the C-terminus of P22 scaffolding protein was responsible for coat protein binding (Tuma et al. 1998). An NMR structure of the C-terminal peptide revealed that a relatively flexible region spanning 27 amino acids between residues 240–267 was followed by a well-defined helix-loop-helix motif spanning residues 268–303 (Fig. 14.2) (Sun et al. 2000). The two helices (helix I – residues 268–283; helix II – residues 289–303) were amphipathic in nature. Hydrophobic residues on each helix are packed together to form a hydrophobic core. The connecting loop consists of five residues (284–288) of which the first four form a type I β-turn. The fifth residue extends the loop allowing the necessary freedom for the helices to associate along their lengths. One striking feature of the structure is the high density of charged residues on the outside of the coat protein-binding domain. Five basic residues (R293, K294, K296, K298, and K300) are located on one side of the outer face of the 12-residue C-terminal helix. The highly charged nature of this surface may form the basis of the observed salt sensitivity of the scaffolding/coat protein interaction.

Directly measuring the strength of the interaction between coat and scaffolding is challenging because rapid assembly complicates the analysis. However, the scaffolding protein can be reversibly removed from and reenter the procapsid. Thus, the binding strength can be measured. Isothermal titration calorimetry provided direct evidence for two classes of scaffolding protein within the procapsid, a tightly bound class and a weakly bound class (Parker et al. 2001). These two classes roughly

correlated with the two rates of scaffolding reentry seen in turbidity-based kinetic assays. The apparent Kd for binding to the high affinity sites was 100–300 nM and was almost entirely enthalpy driven between 10 and 37°C. A more negative than expected ΔCp suggests a conformational change upon binding or that bridging water molecules may be involved.

14.2.6 Auxiliary Functions of P22 Scaffolding Protein

Evidence that the P22 scaffolding protein may facilitate the incorporation of the pilot and portal proteins was first provided by the results of early biochemical characterizations of mutant infections. Procapsid-like particles assembled in the absence of scaffolding protein contained neither of these minor capsid proteins (Earnshaw and King 1978). The isolation of a temperature-sensitive scaffolding protein (S242F), which could drive the assembly of procapsids lacking both portal and pilot proteins, and the isolation of a Y214W mutant, which incorporated pilot proteins but not the portal protein, suggested the central region of the scaffolding protein was involved in these functions. Further support for the role of the central region in minor protein incorporation came from studies utilizing scaffolding protein fragments. Fragments missing the N-terminal 228 amino acids can incorporate portal protein, but the deletion of nine additional residues ablates incorporation (Weigele et al. 2005). Deletion analyses have also defined portal recruitment domains in the HSV-1 (Singer et al. 2005) and Phi29 (Fu et al. 2010) scaffolding proteins suggesting that this may be a general function of scaffolding proteins. Although these findings suggest that the P22 scaffolding protein directly interacts with the portal and minor proteins, no such interactions have been demonstrated biochemically.

14.2.7 The Mechanism of Scaffolding-Assisted Assembly

Any mechanistic model for scaffolding assisted assembly has to accommodate both its role in promoting assembly and ensuring proper form determination. In the assembly of the multishelled bluetongue virus, it has been suggested that the inner core forms a template upon which the outer shell polymerizes (Grimes et al. 1998). While such a mechanism is attractive, it most likely does not operate in the P22 system: no preformed cores of scaffolding protein could be identified under assembly conditions. Initiation of assembly is a critical control point, and it is possible that scaffolding protein might play a role in proper initiation, but it may not be required for further polymerization. However, in vitro experiments with limiting scaffolding protein demonstrated that a minimum of approximately 120 scaffolding proteins is required for assembly, suggesting that it is required throughout the assembly reaction.

Given that scaffolding protein is required for continued polymerization, there are two mechanisms by which it might promote assembly. Scaffolding binding might switch the coat protein subunit from an inactive, unassociable state to one competent for assembly. Alternatively, scaffolding protein might act as an entropy sink. In this model, each of the two coat-binding domains of a scaffolding protein dimer binds one coat protein molecule resulting in the formation of a heterotetramer (two each of scaffolding and coat subunits). Consequently, the effective concentration of coat protein is greatly increased. Thus, the binding energy for scaffolding dimerization is being used to increase the effective concentration of the coat protein. Of course, both mechanisms could be operative at the same time.

The fact that truncated scaffolding protein molecules such as the C-terminal 38 amino acid helix-loop-helix can activate the coat protein for assembly (Tuma et al. 2008) yet do not dimerize suggests that scaffolding binding can activate the coat protein for assembly. However, the breakdown of fidelity observed, with predominately aberrant particles being formed, suggests that the information

required for form determination is not locally transmitted. Based upon a series of N-terminal deletion mutants (WT, Δ1-140, Δ1-237), which show a decreased ability to dimerize, fidelity seems to correlate with dimerization potential though the molecular details of this phenomenon remain obscure (Parker et al. 1998).

14.2.8 Scaffolding Exit from Procapsids

Although scaffolding-containing procapsids are stable structures in which the scaffolding protein can remain bound for prolonged periods of time, they are programmed to release the scaffolding protein intact during DNA packaging. Exit presumably occurs through ~25 Å holes present at the center of the hexameric capsomeres. Whether it is necessary to package some fraction of the DNA to drive egress – as is the case for bacteriophages T4 (Jardine et al. 1998), lambda (Hohn 1983), T3 (Shibata et al. 1987a, b), and T7 (Masker and Serwer 1982) – or whether only DNA/terminase complex docking at the portal vertex is required is unknown. However, circumstantial evidence suggests the former (Poteete et al. 1979). In the case of bacteriophage lambda, there appear to be specific DNA interaction sites within the capsid. Although similar sites have not been identified in P22, their existence seems likely. Parker and Prevelige proposed that scaffolding protein was bound through charge/charge interactions. In this model, the positive charges on the scaffolding proteins' basic C-terminal domain would interact with negatively charged patches on the coat protein subunits (Parker and Prevelige 1998). During DNA packaging, the negative charged DNA would drive the charged patches away from each other, thus promoting capsid expansion and destroying the scaffolding protein binding site. Based on high-resolution structural data, a similar model has recently been proposed for bacteriophage HK97 (Conway et al. 2001).

The NMR structure of the P22 scaffolding protein represented the unbound state, and it is also possible that a conformational change in the scaffolding protein itself contributes to its release. In accord with the suggestion of an active role for scaffolding protein in release, mutational studies have identified regions involved in this function. A deletion of the N-terminal 58 amino acids allows for the production of infectious virions; however, a deletion of an additional five residues halts assembly at the procapsid step. This suggests that residues 58–63 are involved in scaffolding exit. Characterization of the R74C mutant, which confers a temperature-sensitive phenotype, provides further support for an active role in scaffolding egress. At nonpermissive temperatures, the mutant protein halts assembly at the procapsid stage due to the inability of the scaffolding protein to exit. Mutations in herpesvirus scaffolding protein which block scaffolding exit also prevent DNA packaging and maturation (Newcomb et al. 2000).

14.3 The Bacteriophage Phi29 System

The Phi29 system is analogous to the P22 system: its overall life cycle involves prohead assembly, DNA packaging, and scaffolding exit without proteolysis. However, there are two significant differences: (1) five copies of a small RNA molecule (pRNA) must associate with the portal protein for DNA packaging (Guo et al. 1987) and (2) the capsid is elongated or prolate rather than icosahedral procapsid. In the case of Phi29, crystallography has been fruitful, and crystal structures of an assembly naive and released (postassembly) form of the scaffolding protein have been obtained (Morais et al. 2003). The 11-KDa predominately α-helical scaffolding protein forms parallel dimers. The N terminus is folded as a helix-loop-helix, strikingly similar to that seen at the C terminus

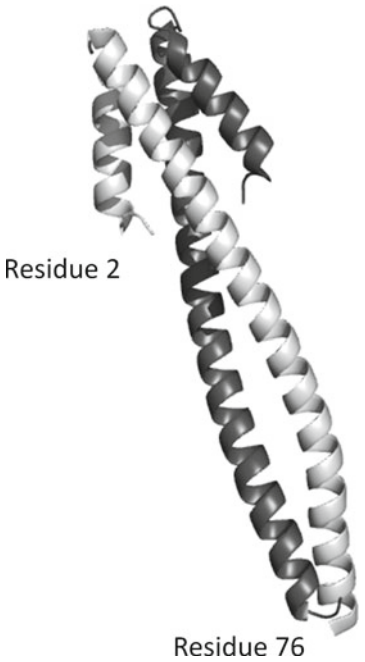

Fig. 14.3 The crystal structure of the Phi29 scaffolding protein dimer. The crystal structure of the preassembly form of the Phi29 scaffolding protein dimer (1NO4) is shown as a *ribbon diagram*. Note the structural similarity of the N terminus of the Phi29 scaffolding protein to the C terminus of the P22 scaffolding protein. The last 15 residues of the Phi29 protein are not seen in the crystal structure

of the P22 scaffolding protein (Fig. 14.3). The helix-loop-helix motifs interact to form an arrowhead-like structure. The shaft of the arrow is formed by a coiled-coil region, and the C-terminal 15 residues are disordered. Despite the structural similarity of the N-terminal region of Phi29 to the C-terminal coat protein binding region of P22, protein dissection experiments indicate that it is the unstructured C terminus of the scaffolding protein that interacts with the coat protein (Fu et al. 2007). Three-dimensional reconstructions of electron micrographs of the procapsid suggest that the scaffolding protein is arranged as a series of four concentric shells that have different symmetries when viewed down the long axis of the prolate icosahedron (Morais et al. 2003). Merging the EM density with the crystal structure suggests that scaffolding protein in the outermost shell selectively interacts with the equatorial coat protein hexamers, which are responsible for the prolate morphology of the procapsid. Evidence for multiple classes of scaffolding protein interactions within the procapsid comes from the observation that the hydrogen/deuterium exchange kinetics are perturbed for some but not all scaffolding protein molecules (Fu and Prevelige 2006). The crystal structure of the released form of the scaffolding protein is very similar to that of the bound form except for a change in the orientation of the last helix relative to the arrowhead (Morais et al. 2003). It is possible that this reorientation of the tail is coupled to scaffolding release.

An in vitro assembly system has also been developed for Phi29. Purified coat and scaffolding subunits can assemble into procapsids (Fu et al. 2007). Strikingly, when portal is included in the reactions, it is also incorporated (Fu and Prevelige 2009). Protein dissection, chemical crosslinking, and mutagenesis experiments have demonstrated that the region of scaffolding protein between amino acids 70–74, which resides adjacent to the unstructured coat-binding region (amino acids 75–98), is responsible for interacting with the portal protein (Fu et al. 2010). Noncovalent mass spectrometry experiments indicate that the scaffolding protein binds to the portal as a dimer and that a maximum of six dimers binds noncooperatively with a Kd of approximately 50 mM (Fu et al. 2010). This complex appears to be capable of nucleating assembly, suggesting a mechanism by which a single portal vertex can be defined during assembly (Fu and Prevelige 2009).

14.4 Scaffolding/Coat Protein Fusions

In contrast to the phages discussed above, some phages encode a scaffolding function located at the N terminus of the coat protein. This domain, known as a delta domain, is required for procapsid assembly but is cleaved by a virus-encoded protease during the transformation to the mature, DNA-containing phage.

14.4.1 HK79

HK97 is a double-stranded DNA-containing bacteriophage whose host is *Escherichia coli* and related bacteria. The structure of the phage capsid was first determined for a tailed bacteriophage (Wikoff et al. 2000), and the subunit fold, which has become known as the HK97 fold, has been found repeatedly in a wide variety of viruses suggesting an evolutionary relationship (Bamford et al. 2005). A remarkable feature of the HK97 capsid is the staged formation of stabilizing isopeptide bonds that covalently cross-link the coat protein subunits into protein chainmail (Wikoff et al. 2000). Similar to P22, the procapsid and capsid are $T=7$ levo structures composed of 415 coat protein subunits and a dodecamer of portal protein at one of the vertices. HK97 does not have a distinct scaffolding protein; instead a 103-amino-acid residue delta domain, located at the N-terminus of the coat protein, fulfills this function (Hendrix and Duda 1998). The delta domain is proteolytically removed following procapsid assembly but prior to DNA packaging. The delta domain itself is highly α-helical in solution. In contrast to many other scaffolding proteins, it does not have a tendency to oligomerize (Nemecek et al. 2009). In the procapsid, the delta domains form inward-projecting clusters, a single cluster can be visualized under the pentamers, while a doublet can be seen under the hexamers (Conway et al. 2007).

14.4.2 T5

The *Siphoviridae* coliphage T5 is distinguished by the large size of its genome and $T=13$ capsid. Like HK97 the genome does not encode a discrete scaffolding protein but rather a delta domain of 159 residues is fused to the N terminus of the coat protein. The delta domain is predicted to be highly α-helical and predominately coiled coil (Effantin et al. 2006). The intact fusion protein, known as pb8p, can assemble in vitro into $T=13$ particles (Huet et al. 2010). Similar to the case with HK97, these particles display inward projecting bundles whose length corresponds to the predicted length of the delta domain. The delta domain occupies most of the internal volume of the procapsid and may act in that manner to fix the size during assembly (Huet et al. 2010).

14.5 The *Microviridae*

14.5.1 The Evolutionary Context of a Dual Scaffolding Protein System

Dual scaffolding protein systems with internal and external species have evolved in both satellite and nonsatellite assembly systems. In satellite systems, typified by bacteriophages P2 and P4 (see below), the external scaffolding protein plays a parasitic role. Encoded by the satellite virus, it

directs helper virus's coat and internal scaffolding proteins into smaller T number capsids, which can only accommodate the smaller satellite virus genome. However, the external scaffolding does not confer new properties to the helper virus coat protein. Most coat proteins that form capsids larger than $T=3$ have retained the ability to form capsids of smaller T numbers (Earnshaw and King 1978; Katsura and Kobayashi 1990; Kellenberger 1990; Newcomb et al. 2001; Stonehouse and Stockley 1993). Thus, the external scaffolding protein alters the thermodynamic barriers that govern the probability of two possible events.

The $T=1$ microviruses, which comprise a subfamily of the *Microviridae*, are nonsatellite viruses that evolved a dual scaffolding protein system. As discussed in the introduction, the necessity of recruiting minor structural proteins to growing capsids may have helped drive the evolution of scaffolding proteins. While this may explain the need for the internal scaffolding protein, which facilitates the incorporation of the minor vertex or DNA pilot protein H, an examination of the niche microviruses occupy is required to understand the evolution of the external scaffolding protein. Microviruses comprise only a small fraction, approximately 3%, of the phages infecting free-living bacteria. They must compete with a vast pool of large dsDNA viruses. The results of evolutionary analyses indicate that the external scaffolding gene, or its most current incarnation, is the most recently acquired microvirus gene (Rokyta et al. 2006). As discussed in greater detail below, the two-scaffolding proteins facilitate a very rapid life cycle (Chen et al. 2007). New progeny appears 5 min postinfection, a time when many dsDNA phages are still in middle gene expression. In contrast, members of the other *Microviridae* subfamily, the one-scaffolding protein gokushoviruses (Clarke et al. 2004), infect obligate intracellular parasitic bacteria. The only known viruses of Chlamydia, these coelacanths take 48 h to replicate (Salim et al. 2008), an affordable luxury when there is no competition.

14.5.2 The Early Stages of øX174 Morphogenesis: Internal Scaffolding Protein-Mediated Reactions

The internal scaffolding protein B mediates the early stages of øX174 morphogenesis. It performs functions reminiscent of other scaffolding proteins, such as ensuring fidelity and minor vertex protein recruitment. As observed in other systems (Desai et al. 1994; Matusick-Kumar et al. 1994, 1995), internal scaffolding–coat protein interactions prevent the aggregation of viral coat proteins into aberrant structures (Siden and Hayashi 1974; Tonegawa and Hayashi 1970). Thus, it confers fidelity to a thermodynamically favorable reaction: the inherent ability of coat proteins to self-associate into curve-surfaced structures.

After coat protein pentamer (9S) formation (Fig. 14.4), five copies of protein B bind to the pentamer's underside and facilitate the incorporation of one copy of the DNA pilot protein H, producing the 9S* particle (Cherwa et al. 2008). As evinced by cryo-EM and crystal models in three rather diverse procapsids, HSV, P22, and øX174, interactions with coat proteins are mostly mediated by the C-termini, which tend to be very ordered and/or exhibit local icosahedral symmetry (Dokland et al. 1997, 1999; Thuman-Commike et al. 1999; Trus et al. 1996; Zhou et al. 1998). Scaffolding protein densities become more diffuse toward the N-termini, suggesting that N-terminal-mediated interactions are much more flexible and variable. Genetic and biochemical data also underscores the critical nature of the C-termini interactions and the flexible nature of the N-termini. Cross-functional analyses have been conducted with scaffolding proteins in both the herpesviruses (BHV-1 and HSV-1) and microviruses (øX174, G4, and α3), and scaffolding proteins can cross-function despite sequence identities as low as 30% (Burch et al. 1999; Haanes et al. 1995). The activity of chimeric scaffolding proteins has also been characterized in both families. For the microviruses, optimal fitness is observed when the C-terminus of the scaffolding protein is of the same origin as the viral coat protein (Burch

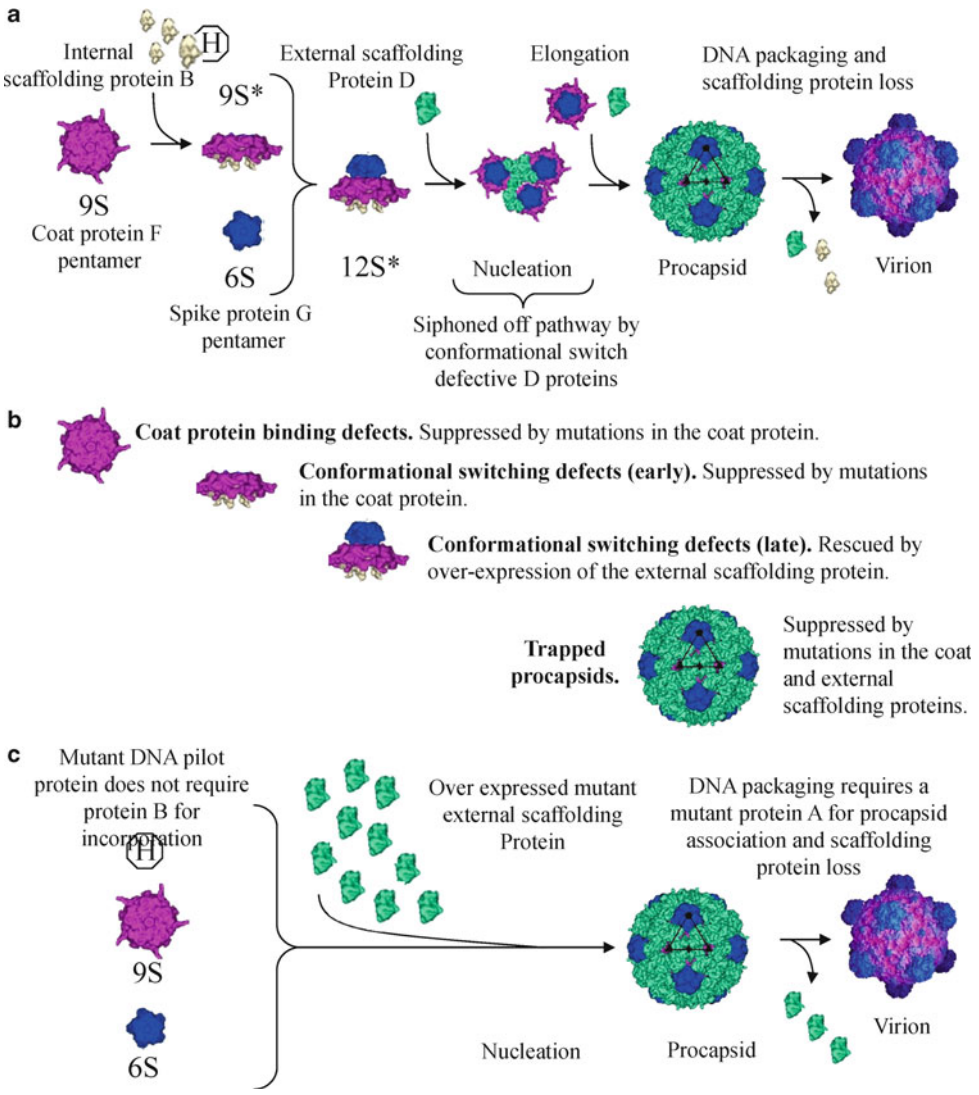

Fig. 14.4 Wild-type, mutant, and B-free øX174 assembly. (**a**) Wild-type assembly pathway. The first identifiable assembly intermediates are pentamers of the viral coat F and major spike G proteins: the respective 9S and 6S particles, which form independently of both scaffolding proteins (Tonegawa and Hayashi 1970). Five internal scaffolding B proteins bind to the underside of the 9S particle, yielding the 9S* intermediate (Cherwa et al. 2008). As *am*(*G*) infections yield particles containing one copy of the DNA pilot protein associated with five copies each of the major capsids F and internal scaffolding B proteins, the DNA pilot protein H may be incorporated at this stage. Protein F–B interactions induce conformational changes on the top of the particle that allows 9S*-6S particle associations, forming the 12S* intermediate (Siden and Hayashi 1974). Twenty external scaffolding D proteins, most likely in the form of five tetramers or ten asymmetric dimers (Morais et al. 2004), interact with the 12S* particle. D–D contacts mediate the construction of the procapsid (108S), an immature virus particle, presumably by allowing pentamers to interact across twofold axes of symmetry (Bernal et al. 2003; Dokland et al. 1997, 1999). (**b**) Particles isolated in cells infected with various B^- mutants. In cells infected with mutants that either do not produce B protein or produce a B protein that cannot bind to coat protein pentamers, 9S* intermediates accumulate. Two phenotypically different classes of B^- conformational switch mutants have been characterized: mutants of one class arrest assembly after the formation of the 9S* particle (early), mutants in the other class after the formation of the 12S* particle. Finally, one mutation has been isolated that produces defective procapsids that cannot be filled. (**c**) The B-free assembly pathway. A sextuple mutant strain of øX174 that can produce particles in the absence of protein B has been isolated (Chen et al. 2007). The 12S* intermediate is circumvented. Procapsid assembly requires the overexpression of a mutant external scaffolding protein. Mutations in protein A and H are also required to produce an infectious virion

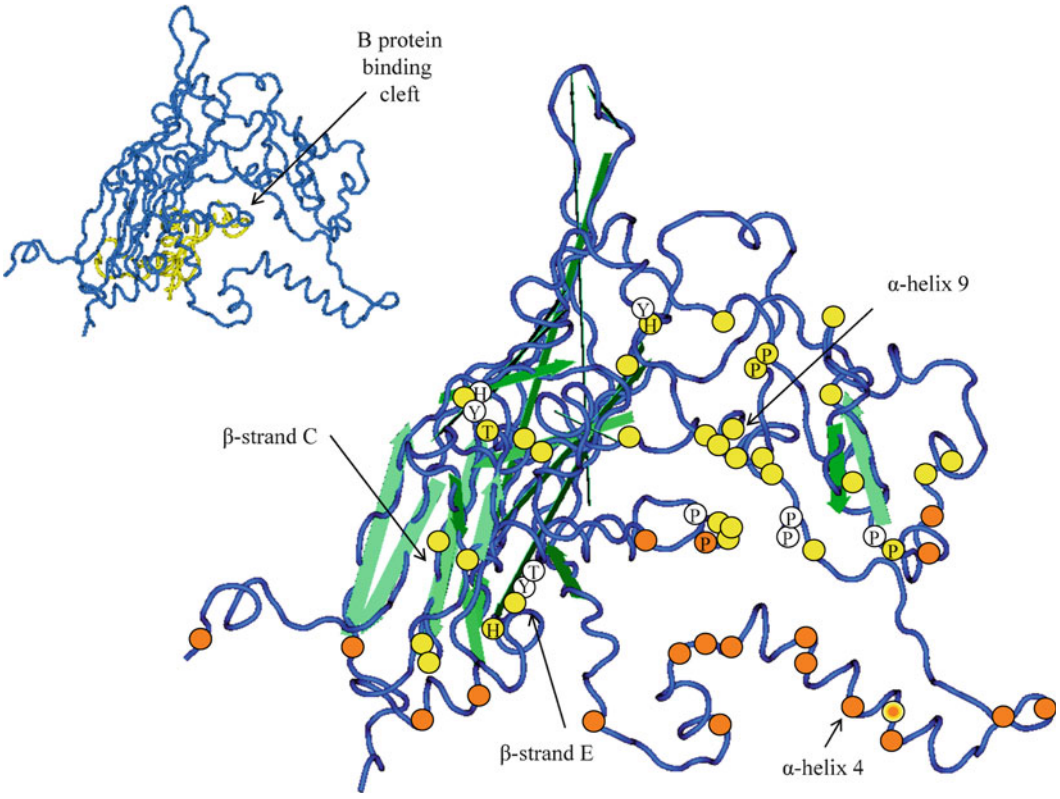

Fig. 14.5 The location of suppressors of mutant external D and internal scaffolding B proteins within the coat protein atomic structure. The suppressors of B^- mutants and mutations that allow the productive utilization of foreign internal scaffolding proteins are indicated with *yellow dots* (Burch et al. 1999; Fane and Hayashi 1991; Gordon, Knuff, Chen, and Fane, unpublished results). All of the parental mutants confer early morphogenetic defects, before the formation of the 12S* particle. The suppressors of D^- mutants and mutations that allow the productive utilization of N-terminal chimeric and deletion scaffolding proteins are indicated with *orange dots* (Fane et al. 1993; Uchiyama and Fane 2005; Uchiyama et al. 2007, 2009). All of the parental mutants confer late morphogenetic defects, post-12S* formation. The *orange–yellow dot* marks the location of the suppressor of a unique B^- protein that produces kinetically trapped procapsids. The location of adjacent proline residues and Thr-X-Tyr-X-X-His motifs is depicted with the letters P and TYH, respectively. Inset: The atomic structures of the coat (*blue*) and internal scaffolding (*yellow*) proteins

and Fane 2000b). Similar results were obtained with chimeric VZV–HSV-1 and CMV–HSV-1 proteins (Oien et al. 1997; Preston et al. 1997). And lastly, procapsid-like structures can be assembled with only C-terminal fragments of the øX174, P22, and P2 scaffolding proteins (Chang et al. 2009; Chen et al. 2007; Tuma et al. 1998; Weigele et al. 2005).

In the absence of the internal scaffolding B protein, coat protein pentamers do not interact with spike protein pentamers (6S particles). Thus, B protein binding to the underside of a 9S particle induces a conformational switch, which alters the pentamer's upper surface. The results of several genetic analyses have identified distinct regions of the coat protein that may participate in these switches. The first analyses, which were conducted before the atomic structure of the procapsid was solved, made use of extant N-terminal missense mutations. These substitutions conferred only weak *cs* (cold sensitive) phenotypes. Their second-site suppressors were located on the coat protein's outer surface and defined five distinct regions, which were characterized by two different primary structure motifs (Fane and Hayashi 1991). One of the motifs was characterized by a Thr-X-Tyr-X-X-His sequence, the other by adjacent proline residues (Fig. 14.5). These sequences may play a key role, perhaps as hinges, in mediating pentamer conformational switches. Mutations in the adjacent

proline residues were also recovered as suppressors that allowed bacteriophage G4 to productively utilize the øX174 scaffolding (Burch et al. 1999) and the øX174 major spike protein (Li and Fane, unpublished results). This latter finding indicates that the ability of coat and spike protein pentamers to associate across species lines and considerable sequence variation during morphogenesis is a function of coat–scaffolding protein interactions.

The inability to isolate missense mutations with nonwild-type phenotypes has hindered investigations of early øX174 morphogenesis. The scarcity of nonwild-type phenotypes most likely reflects the proteins flexible nature, as evinced by the ability of related scaffolding protein to cross-function. "Foreign" scaffolding proteins can be regarded as "multiple mutants." Having diverged as much as 70% on the amino acid level, the dearth of single amino acid substitutions that obliterate function becomes apparent. However, the atomic structure revealed that the vast majority of coat–scaffolding interactions were mediated by just six aromatic amino acids, tyrosines and phenylalanines, in the C terminus of the protein (Dokland et al. 1997, 1999). Using the atomic structure as a guide, a more targeted genetic analysis has begun (Gordon, Knuff, and Fane, unpublished results). Amber mutations were placed at all these sites and four additional sites that do not encode aromatic amino acids. Mutants are then plated on *sup*$^+$ hosts that insert serine, glutamine, or tyrosine during protein synthesis. Thus, the ability to form plaque formation on the various hosts can serve as an indicator of the properties required at a specific site in the protein.

Substitutions of nonaromatic amino acids at the aromatic sites are not tolerated, conferring absolute lethal phenotypes. However, phenotypes differ on the molecular level and affect three distinct stages of early assembly, 9S → 9S* transition, 9S* → 12S* transition, and the 12S* → procapsid transition, suggesting defects in coat protein binding or complex stability. The latter two stages can be regarded as defects in conformational switching. The one mutant that is unable to support the 12S* → procapsid transition is rescued by the exogenous overexpression of the external scaffolding protein, indicating that a higher critical concentration of the external scaffolding protein is required to nucleate procapsids assembly. Second-site suppressors have been isolated for the remaining five of the "missense-suppressed" amber mutations. These suppressors define two hot spots in the coat protein atomic structure (Fig. 14.5), one residing in or adjacent to β-strands C and E and the second throughout α-helix #9, which is adjacent to the B protein binding cleft. In general, most substitutions are tolerated at nonaromatic amino acids. However, the introduction of a tyrosine residue at one of them leads the assembly of kinetically trapped procapsids, which cannot be filled. Unlike the suppressors of other B-mutants, which map to the upper half of the coat protein (Fig. 14.5), its suppressors map to a region of the coat protein rich in mutant external scaffolding protein suppressors (orange–yellow dot in Fig. 14.5).

14.5.3 Functional Redundancy in a Two-Scaffolding Protein System

A more evolutionary approach has been used to elucidate the functions of the internal scaffolding protein. Several lines of evidence suggest that the internal scaffolding protein may be less critical than the external scaffolding protein during morphogenesis. Unlike the internal scaffolding protein, the external scaffolding proteins are highly conserved between microvirus species, more highly ordered in atomic structures, and extremely sensitive to mutation (Dokland et al. 1997, 1999) (Burch and Fane 2000a, 2003; Cherwa et al. 2008). In the two-scaffolding protein P2/P4 satellite system, P4 procapsid-like structures can be generated in vitro from purified external scaffolding and coat proteins (Wang et al. 2000), circumventing the requirement for the internal scaffolding protein, which is required in vivo (Christie and Calendar 1990; Lengyel et al. 1973). However, morphogenesis is not efficient and the reaction is strongly dependent on PEG (Wang et al. 2000), which would effectively raise reactant concentrations via molecular crowding.

After the acquirement of the external scaffolding protein, which appears to be the newest of the microvirus genes (Rokyta et al. 2006), the internal scaffolding protein may have evolved into an "efficiency protein," aiding morphogenetic processes but not strictly required for any one reaction. While its gene was retained in microvirus genomes in an overlapping reading frame (Rokyta et al. 2006), it no longer had a genomic region solely dedicated to its coding as is seen in the gokushovirus genomes (Brentlinger et al. 2002; Liu et al. 2000). Thus, an inherent plasticity would allow other proteins to compensate for reduced or absent B protein function. To test this hypothesis, sequential-targeted selections were performed to reduce the requirement of B protein until it could be completely circumvented (Chen et al. 2007; Novak and Fane 2004). A series of N-terminal deletion B proteins was generated from cloned 5′ deletion genes and used to complement a *nullB* mutant (a nonsense mutation in codon 3). Since the C-terminus is known to mediate most of the known contacts with the viral coat protein (Dokland et al. 1997, 1999), the N-terminus was progressively removed. Proteins with progressively large N-terminal deletions were assayed for complementation on the level of plaque formation, which indicates that the strain could complete the viral life cyle. As the deletions increased in length, complementation became less efficient until it ceased. The deletion protein that failed to complement was then used to select a mutant strain capable of utilizing it. This utilizer mutant was then used for complementation assays with more truncated B proteins, and so forth. Thus, strains have acquired mutations in a sequential manner.

Internal scaffolding proteins lacking the first 53 (Δ53B) of its 120 amino acids can support morphogenesis. The ability to tolerate such a large deletion in a relatively small protein is further evidence that N-terminal functions are moderately expendable and mediate variable interactions with the viral coat protein. However, assembly is very cold sensitive and, most particles produced at permissive temperatures display a lower specific infectivity than wild-type particles due to the inefficient incorporation of the DNA pilot protein H. The recruitment of minor vertex proteins may be a general property of internal scaffolding proteins as similar observations have been made in the P22 system (Weigele et al. 2005). At low temperatures, no procapsids are produced. Substitutions in the external scaffolding protein D suppress the cold-sensitive assembly defect, but do not appear to increase the efficiency of DNA pilot protein H incorporation, which can be overcome by mutations in gene H. The procapsids produced by the Δ58B protein are altered and unable to be filled due to the inability to interact with the DNA-packaging complex. A substitution in the DNA-packaging protein A alleviates this defect. The overexpression of the mutant external scaffolding protein, via a promoter-up mutation, allows procapsids to be assembled with a Δ67B protein. The addition of a coat protein mutation that strengthens coat–external scaffolding proteins is both necessary and sufficient to allow assembly with a Δ97B protein. And finally, the creation of another promoter-up mutation allows plaque formation in the complete absence of protein B, the B-free phenotype. Due to the promoter mutations, viral protein expressions differ greatly in B-free infected cells from that typically observed in wild-type infections. The external scaffolding protein is vastly overproduced relative to the other four structural proteins, which appear to be downregulated. Thus, the ratio between interacting components is dramatically altered to drive procapsid assembly in the absence of the B protein. A summary of B-independent morphogenesis is given in Fig. 14.4.

The B-free phenotype was defined as the ability to form plaques, not the ability to produce progeny, which must occur before programmed cell lysis. It is possible to uncouple plaque formation from virion production by examining progeny production as a function of time in lysis-resistant cells. As can be seen in Fig. 14.6, only the first four of the six mutations found in the B-free mutant are required for progeny production. However, the lag phase before progeny production in vivo was 50 min, long after programmed cell lysis would occur in a lysis-sensitive cell. With the addition of the subsequent mutations, which included more promoter mutations, lag phases became progressively shorter. Thus, one of the primary functions of the internal scaffolding protein is to lower the critical concentration of the external scaffolding protein required to nucleate procapsid morphogenesis. A separate question involves the number of mutations that is required to form an assembled particle, regardless of

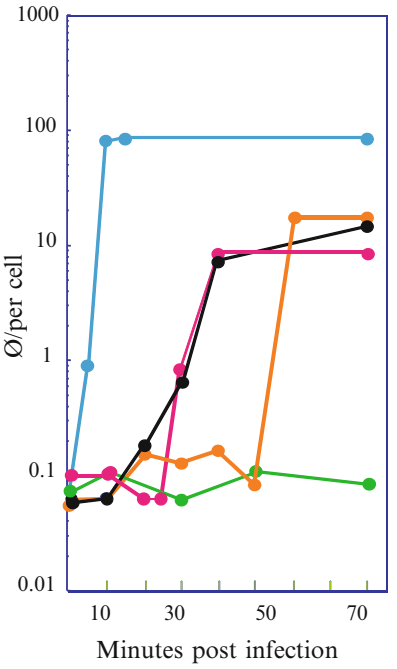

Genotypes and phenotypes of strains

Strain	Mutations1	Plaque Assay Viability	Time of Virion Production
Wild-type		YES	5 min p.i.
NullB Strains:			
Generation 2	A, H, D	$<10^{-6}$	None
Generation 3	A, H, D, P_{D1}	$<10^{-6}$	50 min p.i.
Generation 4	A, H, D, P_{D1}, F	$<10^{-6}$	25 min p.i.
Generation 5	A, H, D, P_{D1}, F, P_{D2}	YES	15 min p.i.

A: DNA packaging and replication protein
H: minor spike protein
D: external scaffolding protein
P_{D1} & P_{D2}: external scaffolding gene promoter
F: capsid protein

Fig. 14.6 Growth kinetics of B-free lineage strains in lysis-resistant cells. The strains used in these experiments were generated in targeted selections designed to produce a multiple mutant that does not require the internal scaffolding protein. Phenotypes and genotypes are given in the figure. Only the generation 5 mutant is viable in plaque assays with lysis-sensitive cells. However, the generation 3 and 4 mutants can produce viable progeny in lysis-resistant cells

infectivity. This may be as low as two. Two of the four mutations in the progeny producing the generation 3 mutant (Fig. 14.6) do not directly involve procapsid proteins. The mutation in protein A is not required to form procapsids, but to package the genome into an altered one. The other mutation is in the D gene promoter. Thus, it is likely that B-independent procapsid assembly only requires a mutation in the DNA pilot protein and the overexpression of a mutant external scaffolding protein.

14.5.4 The External Scaffolding Protein

14.5.4.1 Structure of the Assembled and Unassembled Protein

After 12S* particle formation, 240 copies of the external scaffolding protein D organize 12 12S* particles into a procapsid. The 240 D proteins form an exterior lattice, which bears no resemblance to a $T=4$ capsid. There are four structurally distinct external scaffolding proteins (Dokland et al. 1997, 1999) per asymmetric unit (Fig. 14.7). The four D proteins form dimers of asymmetric dimers (D_1D_2, D_3D_4). Although each subunit has a unique structure, which is partly determined by its unique interactions with the underlying coat protein and neighboring D proteins within and across asymmetric units, there are structurally similarities. The structures of D_1 and D_3 are more similar to each other than to either D_2 or D_4, and the converse is true with the D_2 and D_4 proteins. D_4 has the most unique structure, especially in the arrangement of the N- and C-termini, which appear to be critical for assembly and coat protein recognition (see below). The atomic structure of assembly naive

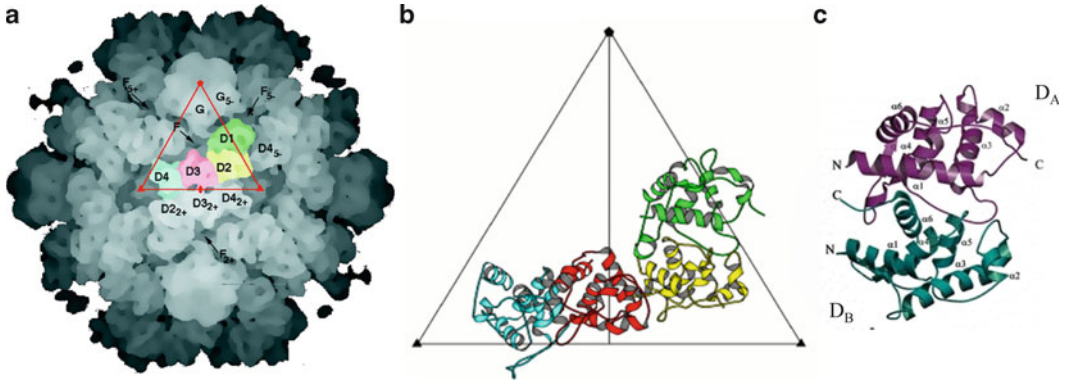

Fig. 14.7 The structure of the øX174 external scaffolding protein D. (**a**) Isosurface tracing of the procapsid illustrating the position of the D_1, D_2, D_3, and D_4 subunits. (**b**) The atomic structure of the D_1, D_2, D_3, and D_4 subunits. The color scheme is identical to that given in part (**a**). (**c**) The atomic structure of the assembly naive D protein dimer, D_AD_B

external scaffolding protein dimer (D_AD_B) has also been solved (Morais et al. 2004). While the D_AD_B dimer structure is unique, it bears a resemblance to the procapsid D_1D_3 and D_2D_4 dimers (Fig. 14.7). The D_A is structurally most similar to D_1 and D_3, while D_B shares a fold closely related to D_2 and D_4. Moreover, the relationship between neighboring asymmetric units in the D_AD_B crystal is similar to that found between the two asymmetric D_1D_2 and D_3D_4 dimers. Thus, the assembly naive subunits are poised to assume the $D_1D_2D_3D_4$ configuration found in the procapsid.

To achieve the unique dimer and tetramer arrangements found in the naive and assembled states, one monomer in each asymmetric dimer (D_1, D_3, or D_A) must be bent. If there were no conformational switch between the monomers, the intra- and interdimer interfaces would be identical. Consequently, the subunits would form a never-ending helix. The conformational switch occurs at glycine residue 61 in α-helix #3, which is bent by 30° in the D_1 and D_3 subunits (Fig. 14.8). Only a glycine residue can accommodate the torsional angle necessary for the D protein to properly adopt one of these two conformations, as the other amino acid side chains occupy forbidden regions of the Ramachandran plot. The organization of the genome further emphasizes the evolutionary importance of maintaining the G61 residue in the external scaffolding protein. Gene E, which encodes the lysis protein, resides entirely within the gene D sequence. Both proteins are translated from the same mRNA, and the G61 and gene E start codons overlap in all known microvirus sequences (Godson et al. 1978; Kodaira et al. 1992; Rokyta et al. 2006; Sanger et al. 1978).

14.5.4.2 Conformational Switching of the External Scaffolding Protein During Assembly

Extensive genetic analyses have been conducted with mutant proteins with substitutions of A, S, T, V, D, K, and P for glycine 61 (Cherwa et al. 2008, 2009; Cherwa and Fane 2009). Mutant genes were constructed on plasmids and assayed for the ability to complement a *nullD* mutant and to inhibit wild-type progeny production. As expected none of the mutant proteins could replace wild-type D protein function in *nullD* infections. In wild-type infections, the mutant proteins inhibit virion morphogenesis, with severity being a function of the substituted amino acid size.

The assembly intermediates made in wild-type and *nullD* infected cells expressing the strongly inhibitory G61D, G61V, and G61P external scaffolding proteins were characterized. In *nullD* infected cells, only the mutant D protein was present and 12S* particles readily accumulated. As the 12S* particle is the last intermediate before the first D protein mediated step in the assembly pathway

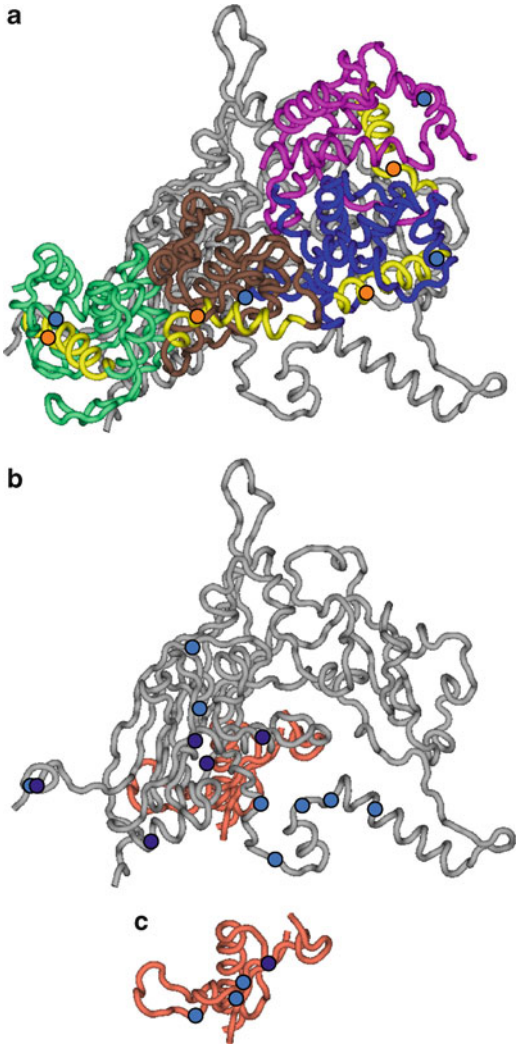

Fig. 14.8 Conformational switch mutants in the external scaffolding protein. (**a**) The location of G61 and D34 residues within the atomic structure of the procapsid. The coat protein is depicted in *gray*, the internal scaffolding protein in peach, and the D_1, D_2, D_3, and D_4 subunits in *magenta*, *blue*, *brown*, and *chartreuse*, respectively. α-helix #3, in which G61 resides (*orange dot*), is colored *yellow*. The helix assumes a straight (D_2 and D_4) or kinked conformation (D_1 and D_3). The location of residue D34 is indicated with a *blue dot*. (**b**) The location of resistance and utilizer mutations in the coat protein. Resistance and utilizer mutations are depicted with *light* and *dark blue dots*, respectively. (**c**) The location of resistance and utilizer mutations in the internal scaffolding protein. All structures are rendered to the same scale and orientation

(Fig. 14.4), the inhibitory proteins behave as if they have no activity vis-à-vis the ability to interact with other assembly intermediates. In wild-type infected cells, both the wild-type and inhibitory proteins would be present. In those infections, 12S* particles do not accumulate but appear to be channeled into off-pathway abominations (Fig. 14.4). As the inhibitory proteins require the wild-type protein to enter into the assembly pathway, the actual inhibitor is most likely a heterodimer.

Mutants resistant to the inhibitory external scaffolding proteins were isolated via direct genetic selections. The resistance mutations conferred amino acid substitution in the coat and internal scaffolding proteins. The affected amino acids cluster beneath or surround the D_3 subunit in the asymmetric unit (Fig. 14.8). The graphics in Fig. 14.8 depict atomic structure of the closed procapsid, which most likely represents an off-pathway product. During crystallization, the coat protein underwent a limited maturation event. In the cryo-electron microscopy reconstruction, which most likely represents the native species, large pores are present at the threefold axes of symmetry (Bernal et al. 2003; Ilag et al. 1995). Thus, the two α-helices that transverse the twofold axis of symmetry would be shifted upward, moving the resistance mutations at amino acids 212, 214, and 227 toward the center of the asymmetric unit. The clustering of the resistance mutations suggests models in which they operate to exclude or accommodate a heterodimer in the D_3D_4 position.

In a structure-based accommodation model, the resistance mutants would be expected to exhibit allele specificity, only accommodating the inhibitory protein for which they were selected. However, they do not exhibit strict allele specificity and even confer resistance against the G61P protein. The G→P substitution would affect the structure of α-helix #3 in a fundamentally different manner than the other substitutions. While the other substitutions would inhibit helix kinking, the proline substitution would lock the helix into a bent position.

While the expression of proteins with more conservative substitutions for G61 (serine and alanine) did not lower wild-type plating efficiencies, wild-type plaque morphologies and burst sizes were reduced. Morphogenesis in *nullD*-infected cells expressing these proteins was examined. Unlike assembly in the absence of D protein, which leads to a pronounced accumulation of 12S* assembly intermediates, particle recovery was skewed toward the recovery of the 9S* intermediate (Cherwa and Fane 2009). This observation may indicate that the G61A and S proteins do not need wild-type subunits to interact with other viral components, as was observed with the G61P, G61V, and G61D proteins. While these data are suggestive, a more compelling argument for G61A and G61S homodimer activity could be made if full complementation could be achieved. Thus, *nullD*/*utilizer* mutants were isolated. The seven *utilizer* mutations resided in the same regions of the coat and internal scaffolding proteins defined by the resistance mutations (Fig. 14.8). Some mutations were identical. *utilizer*/*nullD* virion production was investigated in cells expressing the wild-type and G61S proteins. G61S protein complementation resulted in a longer lag phase. As øX174 has no temporal gene expression, the longer lag phase may indicate that a higher critical concentration of the G61S protein is required to nucleate procapsid morphogenesis. Lower yields and slower rates may reflect secondary defects in the capsid elongation.

14.5.4.3 Inhibitory Proteins and the Evolution of a Three-Scaffolding Protein System

As targeted genetic selections with deletions of the internal scaffolding protein converted øX174 from a two- to a one-scaffolding protein system, the results of experimental evolution studies indicate that it may be possible to evolve a three-scaffolding protein system: one that requires the internal protein and two species of the external protein. The resistance phenotypes conferred by the mutations isolated in one-step genetic selections with the lethal dominant external scaffolding proteins were weak. To isolate a more robust phenotype, which may be predictive of resistant phenotypes that could be selected by prolonged exposure to antiviral agents that specifically target capsid assembly, wild-type øX174 was continually cultured through exponential phase cells expressing an inhibitory D protein (Cherwa et al. 2009). Initially the induction of the inhibitory gene was low, to allow low levels of virus replication. As the viral population began to exhibit increased fitness, indicative of the accumulation of mutant strains, induction levels were steadily increased. After approximately 180 life cycles, a quintuple-mutant resistant strain was isolated from the population. The recovered mutations were very similar to those isolated in one-step genetic selections with the exception of one mutation, which conferred a D→G substitution at amino 34 in α-helix #2 of the external scaffolding protein. As this particular helix mediates no contacts with other structural or scaffolding proteins, the substitution may provide an alternative locus for conformational flexibility, which compensates for the steric hindrance introduced into α-helix #3.

As can be seen in Table 14.1, acquiring resistance to an antiviral agent lowered strain fitness vis-à-vis the uninhibited wild-type levels, a phenomenon that has been observed in other studies (Collins et al. 2004; Paredes et al. 2009; Zhou et al. 2008). Moreover, the resistance strain's replication capacity is higher in the presence of inhibitor. Thus, as observed with other antiviral agents (Baldwin and Berkhout 2007; Salvati et al. 2004), the selection for resistance co-selected for a level of dependence. However, the virus appears to have evolved a mechanism to productively utilize the once

Table 14.1 Fitness (doublings/h) and virion yield (progeny/h/input phage) in continuous culture

	Inhibitory protein expression as percentage of total cellular D protein					
	0%		20%		50%	
Strain	Fitness	Yield	Fitness	Yield	Fitness	Yield
Wild type	9.4 ± 0.3	675	7.4 ± 0.2	170	2.0 ± 0.1	4
Evolved	6.4 ± 0.1	85	12.4 ± 0.1	5,400	5.6 ± 0.5	50

Experiments conducted in replicates of five

inhibitory protein to stimulate its fitness substantially higher than the uninhibited wild-type level, which is a novel phenomenon. Thus, optimal fitness now requires three scaffolding proteins.

The resistant strain was exhaustively characterized to determine the molecular basis of this effect. Although no significant differences in either attachment or eclipse kinetics were observed when compared to the ancestral wild-type strain, the inhibitory protein led to a dramatically shortened lag phase and increase in resistant strain progeny production. The most dramatic effect was observed when the inhibitory protein was present at a 1:3 ratio with the wild-type species. Under these conditions, progeny appears 8 min postinfection, as opposed to 14 min postinfection in the absence of the inhibitor, and progeny production is increased by approximately tenfold. These observations are best explained by the prudent particle – promiscuous protein hypothesis. The inhibitory proteins are known to promiscuously promote off-pathway reactions (Cherwa et al. 2008; Cherwa and Fane 2009); the resistance mutations may produce 12S* intermediates that are less prone to associate with both the inhibitory and wild-type external scaffolding protein. As the dependency phenomenon appears to operate on the level of capsid nucleation, efficient nucleation may now depend on a small concentration of the more promiscuous inhibitory protein.

14.5.4.4 Coat Protein Substrate Specificity Domains in the External Scaffolding Protein

The full extent of coat–external scaffolding protein interactions is not apparent in the atomic structure of the closed procapsid. During crystallization, the particles underwent a limited maturation event, which included a reorganization of the coat protein at the threefold axes of symmetry to generate a closed structure – the native particle contains 30 Å pores in these locations. Moreover, the coat protein pentamers moved inward in a radial manner, forming two- and threefold interactions similar to those observed in the virion, and contacts with the external scaffolding protein are minimal. In contrast, there are very few, if any, cross-pentamer contacts in the cryo-EM model of the native structure, and coat–external scaffolding protein interactions are much more extensive (Bernal et al. 2003; Dokland et al. 1997, 1999; Ilag et al. 1995). However, the results of genetic experiments conducted with chimeric scaffolding proteins have helped elucidate external scaffolding protein domains that confer coat protein specificity (Burch and Fane 2000a, 2003; Uchiyama and Fane 2005; Uchiyama et al. 2007, 2009).

Although most of the primary sequences of microvirus external scaffolding proteins are highly conserved (Godson et al. 1978; Kodaira et al. 1992; Rokyta et al. 2006; Sanger et al. 1978), a considerable degree of sequence divergence is localized to the N- and C-termini of the proteins, which constitute α-helices #1, #7, and loop #6 in the atomic structure. External scaffolding proteins do not cross-function between the related G4, α3, and øX174 species, nor does the expression of a foreign scaffolding protein dramatically interfere with cross-species assembly. However, chimeric øX174/α3 scaffolding proteins with interchanged first α-helices inhibit virion formation in a species-specific manner. Inhibition is observed when the first helix is of the same origin as the viral coat protein (Burch and Fane 2000a). Thus, the incorporation of the inhibitory chimera was a function of the first

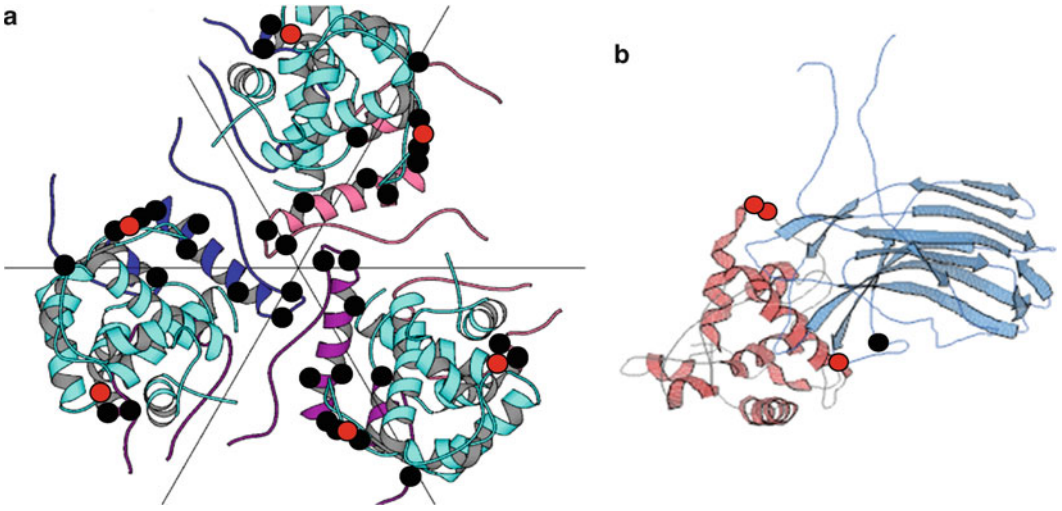

Fig. 14.9 The location of suppressors of chimeric and N-terminal deleted external scaffolding proteins. (**a**) The threefold axis of symmetry in the atomic structure of the closed procapsid. Coat protein sequences are depicted in *dark blue*, *pink*, and *purple*. The external scaffolding protein D_4 subunit is depicted in *light blue*. *Black dots* mark the location of suppressors in the coat protein. *Red dots* indicate the location of the suppressors within the external scaffolding protein. (**b**) Interactions between the external scaffolding protein D_1 subunit and the major spike protein G

α-helix. The results of further biochemical and genetic analyses indicate that the actual inhibitory effects were conferred by the foreign α-helix #7, which resulted in the generation of procapsids that could not be filled (Burch and Fane 2003).

Although the results of the above analysis suggested that α-helix #1 was required for the initial coat–external scaffolding protein recognition, sequence divergence between the øX174 and α3 proteins was too great to obtain mutants that could productively use the chimeric scaffolding proteins. Thus, chimeras between the more closely related G4 and øX174 phages were generated. While the G4/øX174 chimeric scaffolding proteins could not support øX174 *nullD* plaque formation, progeny was produced in lysis-resistant cell after an extended lag phase (Uchiyama and Fane 2005). However, once progeny production initiates, virions appear to be produced at a wild-type rate. Similar results were obtained when the chimeric gene was constructed directly into the viral genome (Uchiyama et al. 2007). These observations suggest that a higher critical concentration of the chimeric protein is required to nucleate virion morphogenesis. Plaque-forming mutants of the chimeric strains were isolated. The mutations shorten the lag phase, allowing progeny production before programmed cell lysis in lysis-sensitive cell. The mutations, along with previous suppressors of cold-sensitive α-helix-1 mutations (Fane et al. 1993), map to two coat protein α-helices that directly surround the threefold axes of symmetry (Figs. 14.5 and 14.9a). Strains with small deletions within the first helix also delay the timing of progeny production. These mutants were also suppressed by substitutions in the external scaffolding as well as by regulatory mutations that elevate the expression level of the N-terminal deleted D proteins (Uchiyama et al. 2009). Again, these results suggest a connection between the lag phase length and the critical concentration needed to nucleate assembly.

While the clustering of the suppressor mutations suggests that interactions between α-helix #1 of the external scaffolding protein and the coat protein helices near the threefold axes of symmetry (Fig. 14.9a) nucleate coat–external scaffolding protein interactions, it is not possible to ascertain which D subunit is involved in this interaction. However, two key structural features suggest the D_4 subunit. It is located at threefold axis of symmetry, and it is the only subunit in which the helix is pointed inward, toward the coat protein. These observations and the atomic structure of the assembly naive D protein dimer suggest a model in which a D_B subunit makes the initial contact with the 12S* particle, interacting with a coat protein in an adjacent fivefold-related asymmetric unit, and becomes

the D_4 protein, as visualized in the procapsid structure. The associated D_A subunit would then sit in the D_3 position. The next D_AD_B dimer to attach would then occupy the D_1D_2 location. However, a secondary site for nucleation may exist. The second-site genetic analyses also identified mutations in the major spike and external scaffolding proteins. The suppressing D protein residues cluster in a loop in the D_1 subunit that extends toward the major spike protein (Fig. 14.9b). The suppressing residue in the major spike protein is in close proximity to α-helix 1 of the D_1 subunit. These suppressors may act by creating an alternate site for initial 12S*–D_AD_B dimer interactions.

14.6 Viruses with Satellites: Reprogramming Size Determination and Molecular Piracy

14.6.1 Bacteriophages P2 and P4

The P2/P4 bacteriophage system represents an example of size determination by the satellite virus P4 encoded external scaffolding protein gpSid (*si*ze *d*etermination). Like many dsDNA viruses, the assembly of the $T=7$ P2 coat protein (gpN) is mediated by its internal scaffolding proteins (gpO) (Christie and Calendar 1990). GpO shares many features with other internal scaffolding proteins. For example, C-terminal fragments are both necessary and sufficient to promote capsid assembly (Chang et al. 2009). However, a small proteolytic fragment of gpO, called O*, remains in the virion (Lengyel et al. 1973; Rishovd and Lindqvist 1992). Like the øX174 internal scaffolding protein (Bernal et al. 2003), gpO is an autoprotease, and the region of the protein responsible for enzymatic activity has been identified (Chang et al. 2009; Wang et al. 2006). It is also likely that gpO is responsible for proteolytic processing of the coat protein (Wang et al. 2006). The satellite bacteriophage encodes the external scaffolding protein sid (*si*ze *d*etermination). In P2/P4 co-infected cells, sid protein alters the curvature of the elongating capsids, which results in a $T=4$ particles. The smaller procapsids cannot accommodate the P2 genome. Thus, they are only filled with the P4 genome.

Structural and genetic studies have somewhat defined the molecular basis of the P4 piracy. The sid–coat protein interactions lead to the formation of a size-restricting cage by influencing the bend of the capsid protein at a flexible hinge region, which was genetically identified by *sir* mutations (*si*d *r*esponsiveness). Sir mutations render the capsid protein resistant to sid protein action (Six et al. 1991). In the cryo-EM model, the sid protein forms a lattice of 12 open pentagons, surrounding the vertices and bifurcating the surrounding hexameric capsomers (Dokland et al. 2002; Marvik et al. 1995) (Wang et al. 2000). The C-termini of sid proteins form trimeric structures at junctions containing three hexamers. Structurally distinct sid dimers interconnect the C-terminal trimer formations. Dimer–dimer and dimer–trimer interactions are most likely mediated via N-termini sid–sid interactions. Extragenic second-site suppressors of *sir* mutations (*nms*), which restore sid sensitivity to *sir* capsid proteins, are located in the C-terminus of the sid protein (Kim et al. 2001). These super-sid proteins most likely form stronger sid trimers, producing a more rigid external lattice that overrides the less flexible hinge regions created by the *sir* mutations. If P4 capsid assembly nucleates with a sid trimer at the junction of three hexamers, the concurrent elongation of the P2 capsid protein with the less flexible and size constraining sid lattice would direct assembly into the smaller $T=4$ capsid.

14.6.2 Phage 80a and Its Parasite SaPI1

In a manner analogous to the P2/P4 system, the *Staphylococcus aureus* pathogenicity island SaPI1, which carries the gene for the toxic shock syndrome toxin, is capable of redirecting the assembly of the phage 80a from a $T=7$ to a smaller $T=4$ procapsids (Spilman et al. 2011; T. Dokland, personal

communication). Mass spectroscopic analysis of the protein composition of the SaPI1 procapsids detected the presence of two SaPI1 proteins, gp6 and gp7 (Poliakov et al. 2008), both of which had previously been implicated in form determination (Ubeda et al. 2008). Both gp6 and gp7 are absent from the mature phage. The NMR structure of purified gp6 indicates that it is structurally similar to the scaffolding protein of Phi29 in that it is highly α-helical, contains an N-terminal helix-loop-helix motif, and is dimeric in solution (T. Dokland, personal communication).

14.7 Concluding Remarks

All scaffolding proteins perform the same basic function: catalyzing and directing capsid assembly, a process that becomes more complicated as icosahedral geometries become more complex. However, as is clearly evident from the case of the $T=1$ microviruses, their performance is finely tuned and optimized by the competitive arena of natural selection. Moreover, many scaffolding proteins have extended their functional repertoire to include controlling the incorporation of other structural proteins, such as portal and pilot proteins, necessary for productive virus infection. Presumably, encoding additional functionality into an existing protein is a cost-effective way to expand function with a minimal increase in genetic load.

Although scaffolding proteins are found in both eukaryotic and prokaryotic viral assembly systems, most mechanistic insights have come from the study of bacteriophages, which are more readily adaptable to laboratory settings. The number of tailed bacteriophages on earth has been estimated to be 10^{31}, and there are an estimated 10^{23} bacterial infections per second (Hendrix 2003). To date we have sampled a small fraction of the continually evolving viruses in the biosphere. It is almost certain that as we sample more deeply, we will find additional and unexpected mechanisms and functions of scaffolding proteins.

References

Baker ML, Jiang W, Rixon FJ, Chiu W (2005) Common ancestry of herpesviruses and tailed DNA bacteriophages. J Virol 79:14967–14970

Baldwin C, Berkhout B (2007) HIV-1 drug-resistance and drug-dependence. Retrovirology 4:78

Bamford DH, Grimes JM, Stuart DI (2005) What does structure tell us about virus evolution? Curr Opin Struct Biol 15:655–663

Berger B, Shor PW, Tucker-Kellogg L, King J (1994) Local rule-based theory of virus shell assembly. Proc Natl Acad Sci USA 91:7732–7736

Bernal RA, Hafenstein S, Olson NH, Bowman VD, Chipman PR, Baker TS, Fane BA, Rossmann MG (2003) Structural studies of bacteriophage alpha3 assembly. J Mol Biol 325:11–24

Bjornsti MA, Reilly BE, Anderson DL (1983) Morphogenesis of bacteriophage phi 29 of *Bacillus subtilis*: oriented and quantized in vitro packaging of DNA protein gp3. J Virol 45:383–396

Brentlinger KL, Hafenstein S, Novak CR, Fane BA, Borgon R, McKenna R, Agbandje-McKenna M (2002) Microviridae, a family divided: isolation, characterization, and genome sequence of phiMH2K, a bacteriophage of the obligate intracellular parasitic bacterium *Bdellovibrio bacteriovorus*. J Bacteriol 184:1089–1094

Burch AD, Fane BA (2000a) Foreign and chimeric external scaffolding proteins as inhibitors of Microviridae morphogenesis. J Virol 74:9347–9352

Burch AD, Fane BA (2000b) Efficient complementation by chimeric Microviridae internal scaffolding proteins is a function of the COOH-terminus of the encoded protein. Virology 270:286–290

Burch AD, Fane BA (2003) Genetic analyses of putative conformation switching and cross-species inhibitory domains in Microviridae external scaffolding proteins. Virology 310:64–71

Burch AD, Ta J, Fane BA (1999) Cross-functional analysis of the Microviridae internal scaffolding protein. J Mol Biol 286:95–104

Casjens S, King J (1974) P22 morphogenesis. I: Catalytic scaffolding protein in capsid assembly. J Supramol Struct 2:202–224

Caspar DLD, Klug A (1962) Physical principles in the construction of regular viruses. Cold Spring Harb Symp Quant Biol 27:1–24

Chang JR, Spilman MS, Rodenburg CM, Dokland T (2009) Functional domains of the bacteriophage P2 scaffolding protein: identification of residues involved in assembly and protease activity. Virology 384:144–150

Chen R, Neill JD, Estes MK, Prasad BV (2006) X-ray structure of a native calicivirus: structural insights into antigenic diversity and host specificity. Proc Natl Acad Sci USA 103:8048–8053

Chen M, Uchiyama A, Fane BA (2007) Eliminating the requirement of an essential gene product in an already very small virus: scaffolding protein B-free oX174, B-free. J Mol Biol 373:308–314

Cherwa JE Jr, Fane BA (2009) Complete virion assembly with scaffolding proteins altered in the ability to perform a critical conformational switch. J Virol 83:7391–7396

Cherwa JE Jr, Uchiyama A, Fane BA (2008) Scaffolding proteins altered in the ability to perform a conformational switch confer dominant lethal assembly defects. J Virol 82:5774–5780

Cherwa JE Jr, Sanchez-Soria P, Wichman HA, Fane BA (2009) Viral adaptation to an antiviral protein enhances the fitness level to above that of the uninhibited wild type. J Virol 83:11746–11750

Christie GE, Calendar R (1990) Interactions between satellite bacteriophage P4 and its helpers. Annu Rev Genet 24:465–490

Clarke IN, Cutcliffe LT, Everson JS, Garner SA, Lambden PR, Pead PJ, Pickett MA, Brentlinger KL, Fane BA (2004) Chlamydiaphage Chp2, a skeleton in the phiX174 closet: scaffolding protein and procapsid identification. J Bacteriol 186:7571–7574

Collins JA, Thompson MG, Paintsil E, Ricketts M, Gedzior J, Alexander L (2004) Competitive fitness of nevirapine-resistant human immunodeficiency virus type 1 mutants. J Virol 78:603–611

Conway JF, Wikoff WR, Cheng N, Duda RL, Hendrix RW, Johnson JE, Steven AC (2001) Virus maturation involving large subunit rotations and local refolding. Science 292:744–748

Conway JF, Cheng N, Ross PD, Hendrix RW, Duda RL, Steven AC (2007) A thermally induced phase transition in a viral capsid transforms the hexamers, leaving the pentamers unchanged. J Struct Biol 158:224–232

Desai P, Watkins SC, Person S (1994) The size and symmetry of B capsids of herpes simplex virus type 1 are determined by the gene products of the UL26 open reading frame. J Virol 68:5365–5374

Dokland T, McKenna R, Ilag LL, Bowman BR, Incardona NL, Fane BA, Rossmann MG (1997) Structure of a viral procapsid with molecular scaffolding. Nature 389:308–313

Dokland T, Bernal RA, Burch A, Pletnev S, Fane BA, Rossmann MG (1999) The role of scaffolding proteins in the assembly of the small, single-stranded DNA virus phiX174. J Mol Biol 288:595–608

Dokland T, Wang S, Lindqvist BH (2002) The structure of P4 procapsids produced by coexpression of capsid and external scaffolding proteins. Virology 298:224–231

Earnshaw W, King J (1978) Structure of phage P22 coat protein aggregates formed in the absence of the scaffolding protein. J Mol Biol 126:721–747

Earnshaw W, Casjens S, Harrison SC (1976) Assembly of the head of bacteriophage P22: x-ray diffraction from heads, proheads and related structures. J Mol Biol 104:387–410

Effantin G, Boulanger P, Neumann E, Letellier L, Conway JF (2006) Bacteriophage T5 structure reveals similarities with HK97 and T4 suggesting evolutionary relationships. J Mol Biol 361:993–1002

Fane BA, Hayashi M (1991) Second-site suppressors of a cold-sensitive prohead accessory protein of bacteriophage phi X174. Genetics 128:663–671

Fane BA, Shien S, Hayashi M (1993) Second-site suppressors of a cold-sensitive external scaffolding protein of bacteriophage phi X174. Genetics 134:1003–1011

Fu CY, Prevelige PE Jr (2006) Dynamic motions of free and bound O29 scaffolding protein identified by hydrogen deuterium exchange mass spectrometry. Protein Sci 15:731–743

Fu CY, Prevelige PE Jr (2009) In vitro incorporation of the phage Phi29 connector complex. Virology 394:149–153

Fu CY, Morais MC, Battisti AJ, Rossmann MG, Prevelige PE Jr (2007) Molecular dissection of o29 scaffolding protein function in an in vitro assembly system. J Mol Biol 366:1161–1173

Fu CY, Uetrecht C, Kang S, Morais MC, Heck AJ, Walter MR, Prevelige PE Jr (2010) A docking model based on mass spectrometric and biochemical data describes phage packaging motor incorporation. Mol Cell Proteomics 9:1764–1773

Fuller MT, King J (1980) Regulation of coat protein polymerization by the scaffolding protein of bacteriophage P22. Biophys J 32:381–401

Godson GN, Barrell BG, Staden R, Fiddes JC (1978) Nucleotide sequence of bacteriophage G4 DNA. Nature 276:236–247

Grimes JM, Burroughs JN, Gouet P, Diprose JM, Malby R, Zientara S, Mertens PP, Stuart DI (1998) The atomic structure of the bluetongue virus core. Nature 395:470–478

Guo PX, Erickson S, Anderson D (1987) A small viral RNA is required for in vitro packaging of bacteriophage phi 29 DNA. Science 236:690–694

Haanes EJ, Thomsen DR, Martin S, Homa FL, Lowery DE (1995) The bovine herpesvirus 1 maturational proteinase and scaffold proteins can substitute for the homologous herpes simplex virus type 1 proteins in the formation of hybrid type B capsids. J Virol 69:7375–7379

Hendrix RW (2003) Bacteriophage genomics. Curr Opin Microbiol 6:506–511

Hendrix RW, Duda RL (1998) Bacteriophage HK97 head assembly: a protein ballet. Adv Virus Res 50:235–288

Hernando E, Llamas-Saiz AL, Foces-Foces C, McKenna R, Portman I, Agbandje-McKenna M, Almendral JM (2000) Biochemical and physical characterization of parvovirus minute virus of mice virus-like particles. Virology 267:299–309

Hogle JM, Chow M, Filman DJ (1985) Three-dimensional structure of poliovirus at 2.9 A resolution. Science 229:1358–1365

Hohn B (1983) DNA sequences necessary for packaging of bacteriophage lambda DNA. Proc Natl Acad Sci USA 80:7456–7460

Huet A, Conway JF, Letellier L, Boulanger P (2010) In vitro assembly of the T = 13 procapsid of bacteriophage T5 with its scaffolding domain. J Virol 84:9350–9358

Ilag LL, Olson NH, Dokland T, Music CL, Cheng RH, Bowen Z, McKenna R, Rossmann MG, Baker TS, Incardona NL (1995) DNA packaging intermediates of bacteriophage phi X174. Structure 3:353–363

Jardine PJ, McCormick MC, Lutze-Wallace C, Coombs DH (1998) The bacteriophage T4 DNA packaging apparatus targets the unexpanded prohead. J Mol Biol 284:647–659

Jiang W, Li Z, Zhang Z, Baker ML, Prevelige PE Jr, Chiu W (2003) Coat protein fold and maturation transition of bacteriophage P22 seen at subnanometer resolutions. Nat Struct Biol 10:131–135

Kang S, Prevelige PE Jr (2005) Domain study of bacteriophage p22 coat protein and characterization of the capsid lattice transformation by hydrogen/deuterium exchange. J Mol Biol 347:935–948

Kang S, Poliakov A, Sexton J, Renfrow MB, Prevelige PE Jr (2008) Probing conserved helical modules of portal complexes by mass spectrometry-based hydrogen/deuterium exchange. J Mol Biol 381:772–784

Katsura I, Kobayashi H (1990) Structure and inherent properties of the bacteriophage lambda head shell. VII. Molecular design of the form-determining major capsid protein. J Mol Biol 213:503–511

Kellenberger E (1990) Form determination of the heads of bacteriophages. Eur J Biochem 190:233–248

Kim KJ, Sunshine MG, Lindqvist BH, Six EW (2001) Capsid size determination in the P2-P4 bacteriophage system: suppression of sir mutations in P2's capsid gene N by supersid mutations in P4's external scaffold gene sid. Virology 283:49–58

King J, Casjens S (1974) Catalytic head assembling protein in virus morphogenesis. Nature 251:112–119

King J, Lenk EV, Botstein D (1973) Mechanism of head assembly and DNA encapsulation in Salmonella phage P22. II. Morphogenetic pathway. J Mol Biol 80:697–731

Kodaira K, Nakano K, Okada S, Taketo A (1992) Nucleotide sequence of the genome of the bacteriophage alpha 3: interrelationship of the genome structure and the gene products with those of the phages, phi X174, G4 and phi K. Biochim Biophys Acta 1130:277–288

Lander GC, Khayat R, Li R, Prevelige PE, Potter CS, Carragher B, Johnson JE (2009) The p22 tail machine at subnanometer resolution reveals the architecture of an infection conduit. Structure 17:789–799

Lebedev AA, Krause MH, Isidro AL, Vagin AA, Orlova EV, Turner J, Dodson EJ, Tavares P, Antson AA (2007) Structural framework for DNA translocation via the viral portal protein. EMBO J 26:1984–1994

Lengyel JA, Goldstein RN, Marsh M, Sunshine MG, Calendar R (1973) Bacteriophage P2 head morphogenesis: cleavage of the major capsid protein. Virology 53:1–23

Lenk E, Casjens S, Weeks J, King J (1975) Intracellular visualization of precursor capsids in phage P22 mutant infected cells. Virology 68:182–199

Liu BL, Everson JS, Fane B, Giannikopoulou P, Vretou E, Lambden PR, Clarke IN (2000) Molecular characterization of a bacteriophage (Chp2) from *Chlamydia psittaci*. J Virol 74:3464–3469

Marvik OJ, Dokland T, Nokling RH, Jacobsen E, Larsen T, Lindqvist BH (1995) The capsid size-determining protein Sid forms an external scaffold on phage P4 procapsids. J Mol Biol 251:59–75

Masker WE, Serwer P (1982) DNA packaging in vitro by an isolated bacteriophage T7 procapsid. J Virol 43: 1138–1142

Matusick-Kumar L, Hurlburt W, Weinheimer SP, Newcomb WW, Brown JC, Gao M (1994) Phenotype of the herpes simplex virus type 1 protease substrate ICP35 mutant virus. J Virol 68:5384–5394

Matusick-Kumar L, Newcomb WW, Brown JC, McCann PJ 3rd, Hurlburt W, Weinheimer SP, Gao M (1995) The C-terminal 25 amino acids of the protease and its substrate ICP35 of herpes simplex virus type 1 are involved in the formation of sealed capsids. J Virol 69:4347–4356

Morais MC, Kanamaru S, Badasso MO, Koti JS, Owen BA, McMurray CT, Anderson DL, Rossmann MG (2003) Bacteriophage phi29 scaffolding protein gp7 before and after prohead assembly. Nat Struct Biol 10: 572–576

Morais MC, Fisher M, Kanamaru S, Przybyla L, Burgner J, Fane BA, Rossmann MG (2004) Conformational switching by the scaffolding protein D directs the assembly of bacteriophage phiX174. Mol Cell 15:991–997
Nemecek D, Overman SA, Hendrix RW, Thomas GJ Jr (2009) Unfolding thermodynamics of the Delta-domain in the prohead I subunit of phage HK97: determination by factor analysis of Raman spectra. J Mol Biol 385:628–641
Newcomb WW, Trus BL, Cheng N, Steven AC, Sheaffer AK, Tenney DJ, Weller SK, Brown JC (2000) Isolation of herpes simplex virus procapsids from cells infected with a protease-deficient mutant virus. J Virol 74: 1663–1673
Newcomb WW, Homa FL, Thomsen DR, Brown JC (2001) In vitro assembly of the herpes simplex virus procapsid: formation of small procapsids at reduced scaffolding protein concentration. J Struct Biol 133:23–31
Novak CR, Fane BA (2004) The functions of the N terminus of the phiX174 internal scaffolding protein, a protein encoded in an overlapping reading frame in a two scaffolding protein system. J Mol Biol 335:383–390
Oien NL, Thomsen DR, Wathen MW, Newcomb WW, Brown JC, Homa FL (1997) Assembly of herpes simplex virus capsids using the human cytomegalovirus scaffold protein: critical role of the C terminus. J Virol 71:1281–1291
Paredes R, Sagar M, Marconi VC, Hoh R, Martin JN, Parkin NT, Petropoulos CJ, Deeks SG, Kuritzkes DR (2009) In vivo fitness cost of the M184V mutation in multidrug-resistant human immunodeficiency virus type 1 in the absence of lamivudine. J Virol 83:2038–2043
Parent KN, Doyle SM, Anderson E, Teschke CM (2005) Electrostatic interactions govern both nucleation and elongation during phage P22 procapsid assembly. Virology 340:33–45
Parker MH, Prevelige PE Jr (1998) Electrostatic interactions drive scaffolding/coat protein binding and procapsid maturation in bacteriophage P22. Virology 250:337–349
Parker MH, Stafford WF 3rd, Prevelige PE Jr (1997) Bacteriophage P22 scaffolding protein forms oligomers in solution. J Mol Biol 268:655–665
Parker MH, Casjens S, Prevelige PE Jr (1998) Functional domains of bacteriophage P22 scaffolding protein. J Mol Biol 281:69–79
Parker MH, Brouillette CG, Prevelige PE Jr (2001) Kinetic and calorimetric evidence for two distinct scaffolding protein binding populations within the bacteriophage P22 procapsid. Biochemistry 40:8962–8970
Poh SL, el Khadali F, Berrier C, Lurz R, Melki R, Tavares P (2008) Oligomerization of the SPP1 scaffolding protein. J Mol Biol 378:551–564
Poliakov A, Chang JR, Spilman MS, Damle PK, Christie GE, Mobley JA, Dokland T (2008) Capsid size determination by *Staphylococcus aureus* pathogenicity island SaPI1 involves specific incorporation of SaPI1 proteins into procapsids. J Mol Biol 380:465–475
Poteete AR, Jarvik V, Botstein D (1979) Encapsulation of phage P22 DNA in vitro. Virology 95:550–564
Preston VG, Kennard J, Rixon FJ, Logan AJ, Mansfield RW, McDougall IM (1997) Efficient herpes simplex virus type 1 (HSV-1) capsid formation directed by the varicella-zoster virus scaffolding protein requires the carboxy-terminal sequences from the HSV-1 homologue. J Gen Virol 78(Pt 7):1633–1646
Prevelige PE Jr, Thomas D, King J (1988) Scaffolding protein regulates the polymerization of P22 coat subunits into icosahedral shells in vitro. J Mol Biol 202:743–757
Prevelige PE Jr, Thomas D, King J (1993) Nucleation and growth phases in the polymerization of coat and scaffolding subunits into icosahedral procapsid shells. Biophys J 64:824–835
Rao VB, Feiss M (2008) The bacteriophage DNA packaging motor. Annu Rev Genet 42:647–681
Rishovd S, Lindqvist B (1992) Bacteriophage P2 and P4 morphogenesis: protein processing and capsid size determination. Virology 187:548–554
Rokyta DR, Burch CL, Caudle SB, Wichman HA (2006) Horizontal gene transfer and the evolution of microvirid coliphage genomes. J Bacteriol 188:1134–1142
Rossmann MG (1984) Constraints on the assembly of spherical virus particles. Virology 134:1–11
Salim O, Skilton RJ, Lambden PR, Fane BA, Clarke IN (2008) Behind the chlamydial cloak: the replication cycle of chlamydiaphage Chp2, revealed. Virology 377:440–445
Salvati AL, De Dominicis A, Tait S, Canitano A, Lahm A, Fiore L (2004) Mechanism of action at the molecular level of the antiviral drug 3(2H)-isoflavene against type 2 poliovirus. Antimicrob Agents Chemother 48:2233–2243
Sanger F, Coulson AR, Friedmann T, Air GM, Barrell BG, Brown NL, Fiddes JC, Hutchison CA 3rd, Slocombe PM, Smith M (1978) The nucleotide sequence of bacteriophage phiX174. J Mol Biol 125:225–246
Shibata H, Fujisawa H, Minagawa T (1987a) Early events in DNA packaging in a defined in vitro system of bacteriophage T3. Virology 159:250–258
Shibata H, Fujisawa H, Minagawa T (1987b) Characterization of the bacteriophage T3 DNA packaging reaction in vitro in a defined system. J Mol Biol 196:845–851
Siden EJ, Hayashi M (1974) Role of the gene beta-product in bacteriophage phi-X174 development. J Mol Biol 89:1–16
Simpson AA, Tao Y, Leiman PG, Badasso MO, He Y, Jardine PJ, Olson NH, Morais MC, Grimes S, Anderson DL, Baker TS, Rossmann MG (2000) Structure of the bacteriophage phi29 DNA packaging motor. Nature 408: 745–750

Singer GP, Newcomb WW, Thomsen DR, Homa FL, Brown J (2005) Identification of a region in the herpes simplex virus scaffolding protein required for interaction with the portal. J Virol 79:132–139

Six EW, Sunshine MG, Williams J, Haggard-Ljungquist E, Lindqvist BH (1991) Morphopoietic switch mutations of bacteriophage P2. Virology 182:34–46

Spilman MS, Dearborn AD, Chang JR, Damle PK, Christie GE, Dokland TA (2011) Conformational switch involved in maturation of *Staphylococcus aureus* bacteriophage 80 alpha capsids. J Mol Biol 405:863–876

Stonehouse NJ, Stockley PG (1993) Effects of amino acid substitution on the thermal stability of MS2 capsids lacking genomic RNA. FEBS Lett 334:355–359

Sun Y, Parker MH, Weigele P, Casjens S, Prevelige PE Jr, Krishna NR (2000) Structure of the coat protein-binding domain of the scaffolding protein from a double-stranded DNA virus. J Mol Biol 297:1195–1202

Tang J, Johnson JM, Dryden KA, Young MJ, Zlotnick A, Johnson JE (2006) The role of subunit hinges and molecular "switches" in the control of viral capsid polymorphism. J Struct Biol 154:59–67

Thuman-Commike PA, Greene B, Jakana J, Prasad BV, King J, Prevelige PE Jr, Chiu W (1996) Three-dimensional structure of scaffolding-containing phage p22 procapsids by electron cryo-microscopy. J Mol Biol 260:85–98

Thuman-Commike PA, Greene B, Malinski JA, Burbea M, McGough A, Chiu W, Prevelige PE Jr (1999) Mechanism of scaffolding-directed virus assembly suggested by comparison of scaffolding-containing and scaffolding-lacking P22 procapsids. Biophys J 76:3267–3277

Tonegawa S, Hayashi M (1970) Intermediates in the assembly of phi X174. J Mol Biol 48:219–242

Trus BL, Booy FP, Newcomb WW, Brown JC, Homa FL, Thomsen DR, Steven AC (1996) The herpes simplex virus procapsid: structure, conformational changes upon maturation, and roles of the triplex proteins VP19c and VP23 in assembly. J Mol Biol 263:447–462

Tuma R, Parker MH, Weigele P, Sampson L, Sun Y, Krishna NR, Casjens S, Thomas GJ Jr, Prevelige PE Jr (1998) A helical coat protein recognition domain of the bacteriophage P22 scaffolding protein. J Mol Biol 281:81–94

Tuma R, Tsuruta H, French KH, Prevelige PE (2008) Detection of intermediates and kinetic control during assembly of bacteriophage P22 procapsid. J Mol Biol 381:1395–1406

Ubeda C, Maiques E, Barry P, Matthews A, Tormo MA, Lasa I, Novick RP, Penades JR (2008) SaPI mutations affecting replication and transfer and enabling autonomous replication in the absence of helper phage. Mol Microbiol 67:493–503

Uchiyama A, Fane BA (2005) Identification of an interacting coat-external scaffolding protein domain required for both the initiation of phiX174 procapsid morphogenesis and the completion of DNA packaging. J Virol 79:6751–6756

Uchiyama A, Chen M, Fane BA (2007) Characterization and function of putative substrate specificity domain in microvirus external scaffolding proteins. J Virol 81:8587–8592

Uchiyama A, Heiman P, Fane BA (2009) N-terminal deletions of the phiX174 external scaffolding protein affect the timing and fidelity of assembly. Virology 386:303–309

Verlinden Y, Cuconati A, Wimmer E, Rombaut B (2000) Cell-free synthesis of poliovirus: 14S subunits are the key intermediates in the encapsidation of poliovirus RNA. J Gen Virol 81:2751–2754

Wang S, Palasingam P, Nokling RH, Lindqvist BH, Dokland T (2000) In vitro assembly of bacteriophage P4 procapsids from purified capsid and scaffolding proteins. Virology 275:133–144

Wang S, Chang JR, Dokland T (2006) Assembly of bacteriophage P2 and P4 procapsids with internal scaffolding protein. Virology 348:133–140

Weigele PR, Sampson L, Winn-Stapley D, Casjens SR (2005) Molecular genetics of bacteriophage P22 scaffolding protein's functional domains. J Mol Biol 348:831–844

Wikoff WR, Liljas L, Duda RL, Tsuruta H, Hendrix RW, Johnson JE (2000) Topologically linked protein rings in the bacteriophage HK97 capsid. Science 289:2129–2133

Zhou ZH, Macnab SJ, Jakana J, Scott LR, Chiu W, Rixon FJ (1998) Identification of the sites of interaction between the scaffold and outer shell in herpes simplex virus-1 capsids by difference electron imaging. Proc Natl Acad Sci USA 95:2778–2783

Zhou Y, Bartels DJ, Hanzelka BL, Muh U, Wei Y, Chu HM, Tigges AM, Brennan DL, Rao BG, Swenson L, Kwong AD, Lin C (2008) Phenotypic characterization of resistant Val36 variants of hepatitis C virus NS3-4A serine protease. Antimicrob Agents Chemother 52:110–120